ELSEVIER

Thin Solid Films 400 (2001) 9–15

thin Solid films

www.elsevier.com/locate/tsf

Ultrathin oxide films on metals: new physics and new chemistry?

S. Altieri[a,*], L.H. Tjeng[b], G.A. Sawatzky[b]

[a]*Istituto Nazionale per la Fisica della Materia, via G. Campi 213/a, I-41100 Modena, Italy*
[b]*Solid State Physics Laboratory, Materials Science Centre, University of Groningen, Nijenborgh 4, 9747 AG Groningen, The Netherlands*

Abstract

Oxide thin films on metals are now currently used as model systems to study the surface properties of highly insulating oxides by means of electron spectroscopies. However, it has been recently proposed that ultrathin oxide films and oxide–metal interfaces may actually have unprecedented intrinsic chemical–physical properties, because of image potential screening of charge fluctuations and interfacial hybridizational effects. In fact, on-site Coulomb interactions and charge transfer energies in oxide thin films on metals are reduced by as much as a few eV as compared to the bulk values, thus suggesting a large reduction of the conductivity gap and a strong enhancement of the strength of various exchange and superexchange magnetic interactions in thin layers of strongly correlated oxides on metals. Moreover, interfacial oxygen states with strong metallic character have been observed and considered responsible for an unusually high and chemical selective reactivity of oxide–metal interfaces. Some basic ideas and results connected with these intriguing interfacial phenomena will be presented and discussed taking MgO thin films on Ag(100) as a model system.

Keywords: Ultrathin oxide films; Oxide-metal interfaces; Coulomb interactions; MgO thin films

1. Introduction

Oxide thin films on metallic substrates provide a possible way out to dramatic charging problems which severely hamper the study of wide band gap insulators by electron spectroscopy and other surface science techniques based on electrically charged probes. For this reason, in recent years there has been an increasing interest in the preparation and characterization of metal supported oxide films which are by now widely employed as model systems to study the surface properties of highly insulating oxides [1–4].

Nevertheless, it has been recently proposed that ultrathin oxide films and oxide–metal interfaces may actually have unprecedented intrinsic chemical–physical properties, because of image potential screening of charge fluctuations and interfacial hybridizational effects. This can be understood realizing that the basic electronic structure, band gaps and superexchange interactions, in strongly correlated oxides are mostly determined by a few fundamental quantities, and that among these the on-site Coulomb interactions U in the open cation shell, and the corresponding multiplet structure, the charge transfer energy Δ, i.e. the energy cost to transfer one electron from the O 2p to the cation shell, and the one-electron band widths, are the most important ones. When U and Δ are larger than the band width, the oxide will be a magnetic insulator, for which the nature and the magnitude of the conductivity gap are determined by the relative importance of U and Δ. Therefore, if ways could be found to strongly reduce U and Δ, then the material might go through an insulator-metal phase transition. Moreover, even for modest reductions of U and Δ, the strength of the exchange interactions, which are inversely proportional to U and Δ, will be considerably enhanced. When the one electron band widths are larger than U and Δ, then the effects of electron correlation become negligible and the material's properties are mostly determined by electron delocalization and hybridization effects. However, at oxide–metal interfaces new hybridizational interactions may set in, so that also the properties of non-correlated oxide thin

* Corresponding author: Tel.: +39-059-205-5242; fax: +39-059-367-488.
E-mail address: altieri@unimo.it (S. Altieri).

0040-6090/01/$ - see front matter
PII: S0040-6090(01)01484-5

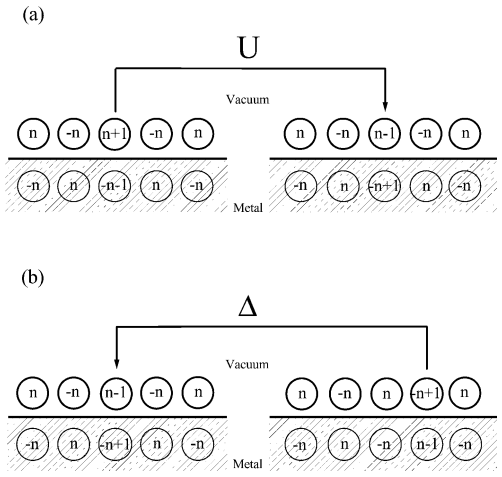

Fig. 1. Combined electron removal and addition process for a thin ionic film close to a metal surface, defining (a) the Coulomb interaction U at the cation site and (b) the anion-to-cation charge transfer energy Δ. In the ground state, the valence of the open-shell cation is (n) and that of the anion is $(-n)$. The ionic charges are subjected to the interaction with the metal which can be represented as an interaction with image charges. During the charge excitation process additional opposite image charges appear below the surface, thereby reducing U by $2E_{\text{image}}$. Also Δ is reduced by $2E_{\text{image}}$ if the Δ of the double film (i.e. film plus *static* mirror film) is taken as a reference.

films in the vicinity of a metal surface might be significantly modified.

In the present paper we shall discuss the possibility that ultrathin oxide films on metals may have unprecedented chemical–physical properties due to modified electronic and magnetic structure by the mutual interaction with the metal surface. The case of strongly correlated and non-correlated oxides will be discussed separately.

2. Strongly correlated oxide thin films on metals

2.1. A 'gedanken experiment'

One possible way of changing U and Δ of a correlated oxide is to grow the oxide as a thin film on a metal substrate or as an oxide–metal multilayer. Duffy and Stoneham [5] predicted that in such a case the image potential will enter the energetics of the system and reduce U considerably. This is illustrated in Fig. 1a, showing an ionic lattice for which the U on the open-shell cation site is defined as the energy required for the charge excitation $2(n)\rightarrow(n+1)+(n-1)$, where (n) is the valence of the cation in the ground state. U for a lattice of isolated ions is given by:

$$U = E_I^{\text{cat}} - E_A^{\text{cat}} \tag{1}$$

where E_I^{cat} is the ionization potential and E_A^{cat} the electron affinity of the cation. Close to the metal surface, all the ionic charges are subject to the interaction with the metal that can be described as an effective interaction with *image charges* appearing below the metal surface. The creation of the additional positive (negative) charge on the cation is then accompanied effectively by the simultaneous creation of an additional negative (positive) image charge in the metal. The energy of the charge excitation that defines U is given by the total energy of two cations with charges $(n+1)$ and $(n-1)$, minus the total energy of the cations in the ground state with both charges (n) and in the presence of image charges is altered into:

$$U = E_I^{\text{cat}} - E_A^{\text{cat}} - (n+1)^2 E_{\text{image}} - (n-1)^2 E_{\text{image}} + 2n^2 E_{\text{image}} \tag{2}$$

where the third and fourth terms describe the total image charge stabilization energy of the two cations in the excited state, and the fifth term that of the two cations in the ground state. Here E_{image} is defined as the binding energy of a unit charge with its induced image charge, and is a positive quantity. The result is now that U is reduced by two times the unit image charge energy, i.e.

$$U = E_I^{\text{cat}} - E_A^{\text{cat}} - 2E_{\text{image}} \tag{3}$$

We argue that Δ will also be similarly reduced and could be smaller than in the bulk depending on the change in the Madelung potential. This is illustrated in Fig. 1b, showing the charge excitation that defines Δ, namely $(n)+(-n)\rightarrow(n-1)+(-n+1)$, where (n) is the valence of the cation and $(-n)$ of the anion in the ground state. The energy cost is given by:

$$\Delta = -E_A^{\text{cat}} + E_I^{\text{an}} - e\sum_{i\neq 0} V_i - e\sum_{i'\neq 0} V_{i'} + e\sum_{j\neq 0} V_j + e\sum_{j'\neq 0} V_{j'} - 2(n-1)^2 E_{\text{image}} + 2n^2 E_{\text{image}} \tag{4}$$

Here the third and fourth terms describe the cost in energy when an electron (with charge $-e$) is added at the cation site $(i=0)$ due to the Madelung potential set up by all other ions $(i\neq 0)$ and their images $(i'\neq 0)$, i.e. the image of the cation excluded). Similarly, the fifth and sixth terms are the cost in energy when an electron is removed from the anion site $(j=0)$ due to the Madelung potential set up by all other ions $(j\neq 0)$ and their images $(j'\neq 0)$. The last two terms represent the change in the stabilization energy in the final and the ground states due to the image charges of the cation and anion involved in the charge excitation process considered. We note that the image charges of all the other ions are static with respect to the excitation, and that therefore their energy contributions can be described as originating from a Madelung like potential. Realizing now that, for the cation $-eV_{i'=0}=2nE_{\text{image}}$ and that for the anion $eV_{j'=0}=2nE_{\text{image}}$, where the factor of two accounts for the fact that the energy associated with an induced charge is half that for a static charge, the expression for Δ can be rewritten as:

$$\Delta = -E_A^{\mathrm{cat}} + E_I^{\mathrm{an}} - e\sum_{i\neq 0} V_i - e\sum_{i'} V_{i'} + e\sum_{j\neq 0} V_j + e\sum_{j'} V_{j'} - 2E_{\mathrm{image}} \quad (5)$$

In other words, the Madelung potentials that contribute to Δ for a thin ionic film on a metal are now equal to those for a double film consisting of the ionic film plus its *static* image film. Thus, if the Madelung potentials of such a double film are not too different from those in the bulk material, the Δ of a thin film on a metal will be smaller by $2E_{\mathrm{image}}$ as compared to that of the bulk.

2.2. Reduction of Coulomb interactions and charge transfer energies

In the last decade, there has been an increasing amount of effort to understand theoretically the properties of oxide–metal interfaces. Far away from the interface, i.e. at distances large compared to the inter atomic lattice spacing, it is expected that a continuum dielectric approximation can provide an accurate description. Very close to the interface, however, the atomistic nature of the metal surface cannot be neglected anymore. It has been suggested, for instance, that the finite wavelength response of the metal surface due to the existence of a Fermi surface introduces strong deviations from the classical electrodynamics results. An experimental determination of U and Δ for oxide films in close vicinity to metal surfaces is therefore highly desired. It is, however, also a difficult task, because the charge fluctuations in correlated electron systems created, for instance, in a spectroscopic experiment, involve not only the transition metal (TM) 3d degrees of freedom but also simultaneously transfer of charge from the O 2p to the TM 3d. The interpretation of the data is, therefore, not so straightforward and requires detailed calculations. To avoid these difficulties, we have recently conducted a spectroscopic investigation of ultrathin MgO(100) films epitaxially grown on a Ag(100) substrate [6], thereby making use of the finding that MgO(100) films can be grown epitaxially on the Ag(100) surface in a well controlled manner [7]. With its crystal structure similar to some TM oxides, MgO may serve as a model system without the complexity due to correlation effects because of its closed shell electronic structure. It allows for the direct determination of changes in U and Δ via a combined X-ray photoemission (XPS) and Auger electron spectroscopy (AES) experiment. In fact, from the energy conservation principle, the following equation can be written down:

$$E_{\mathrm{kin}}^{\mathrm{KLL}} = E_b^{1\mathrm{s}} - 2E_b^{2\mathrm{p}} - U \quad (6)$$

where $E_{\mathrm{kin}}^{\mathrm{KLL}}$ is the kinetic energy of a KLL Auger transition, and $E_b^{1\mathrm{s}}$ and $E_b^{2\mathrm{p}}$ denote the 1s and 2p XPS core level binding energies, respectively. Measuring the

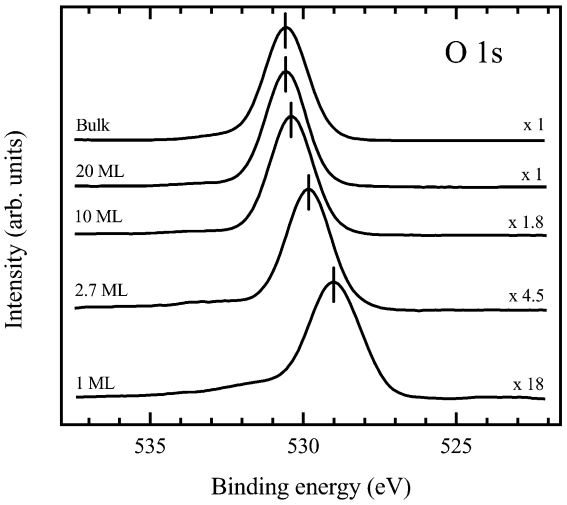

Fig. 2. O 1s core level XPS spectra of bulk MgO and MgO(100) films on Ag(100). The core level of the 10, 2.7 and 1 ML film shifts towards lower binding energies by 0.2, 0.8 and 1.6 eV, respectively, relative to that of the 20 ML film.

XPS and Auger spectra of Mg in the thin MgO films on Ag(100), and using Eq. (6), we found [6] that U indeed becomes smaller as the thickness of the film is reduced. Relative to the bulk or to the 20-ML film, the reduction of U amounts to 0.4, 0.8 and 1.8 eV (± 0.2 eV) for thicknesses of 10, 2.7 and 1 ML, respectively. These observations fit well with the expectations based on the simple model presented in Fig. 1. They also show that the effects due to the presence of the oxide–metal interface are quite appreciable and still operative at coverages as high as 10 ML.

A similar analysis can be carried out for the Coulomb interaction U in the O 2s and 2p shells using the O KL_1L_1 and $KL_{23}L_{23}$ Auger data, respectively, and the corresponding oxygen XPS core levels as reported in Figs. 2 and 3. The results reveal that also the oxygen Coulomb interactions are reduced in the thinner films. The reduction of U is approximately 1.3 eV, for both the O 2s and 2p shells. The uncertainty in this number is, however, larger than in the U of the Mg 2p shell. We estimate that the margin of error in the reduction of U in the O 2s is approximately ± 0.5 eV, due to the uncertainty with which the peak position of the extremely low intensity O KL_1L_1 Auger line of the 1 ML MgO(100) can be determined. The error in the reduction of U in the O 2p is also at least ± 0.5 eV, but for a different reason. Here, the O $2p^4$ final state of the $KL_{23}L_{23}$ Auger process can hybridize with states in which one of the two holes have hopped to a neighboring orbital [8] causing changes in the Auger peak positions that have not been taken into account by the simple model as given by Eq. (6). It is important to realize that these hybridizational effects are quite different for the 1 ML case as compared to the bulk, since

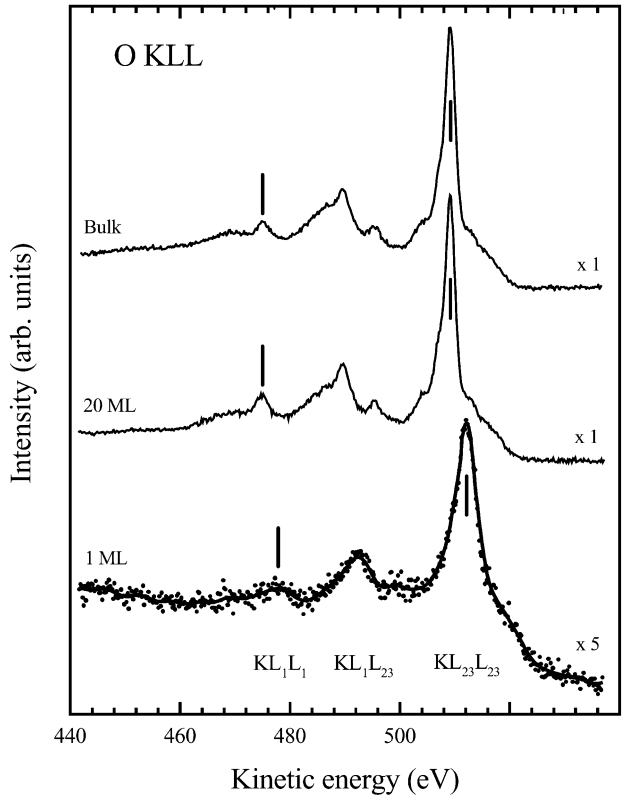

Fig. 3. O KL_1L_1, KL_1L_{23}, and $KL_{23}L_{23}$ Auger spectra of bulk MgO and MgO(100) films on Ag(100). A shift towards higher kinetic energies by approximately 2.9 eV can be observed for the 1 ML spectra with respect to the 20 ML and bulk spectra.

the O 2p orbital of the monolayer can mix not only with neighboring O 2p orbitals but also with the underlying Ag 4d and 5sp bands. This is indicated, for instance, by the much larger FWHM of the O $KL_{23}L_{23}$ Auger line in the 1 ML film as shown in Fig. 3.

Also the changes in the charge transfer energy Δ with the film thickness can be defined in terms of the measured core level binding energy shifts, plus the previously obtained reductions of U [6]. In doing so one then finds that also Δ becomes smaller for thinner films [6]. Compared to bulk MgO or to the 20 ML film, Δ is reduced by approximately 0.5, 1.2 and 2.5 eV in the 10, 2.7 and 1 ML film, respectively. However, while the reduction of the Coulomb interaction U with the film thickness depends only upon the changes in the total relaxation energy [6], the changes in Δ also depend on the changes in the Madelung potential (for example due to changes in the coordination number) since the charge fluctuations defining Δ involve two times the Madelung potential energy. For the 10 ML and the 2.7 ML case, we expect the changes in the Madelung potential to be negligible, since the contribution to the Madelung potential from layers that are farther away than two interlayer spacing is already less than 0.05% (see Table 1). The reduction in Δ can therefore be attributed to the increase in the extra-atomic relaxation energies at both the O and the Mg sites due to the close proximity of the Ag metal surface [6]. For the 1-ML thick film, however, the Madelung potential, as discussed below, is appreciably changed from the bulk value, and thus significantly contributes to reduce Δ.

The observed reduction of U and Δ implies that the electrical, magneto-optical, and transport properties of, for example, transition metal oxides, will be strongly modified if they are deposited as thin films on a metal substrate. Consider for instance a magnetic insulator with an electronic structure which can be described by an effective half-filled Hubbard model. The interatomic exchange interactions are then given by , where t denotes the inter-site hopping integral, and they will be strongly enhanced near the interface with a metal since U is reduced. Similarly, the oxygen mediated superexchange interactions $J \approx [-2t^4/\Delta^2] \times [(1/\Delta) + (1/U)]$ important in many rock-salt and perovskite transition metal structures, might be greatly enhanced in ultrathin films on a metal, because of the cooperative effect of the reduced U and Δ. This means that, among others, the critical temperatures for various forms of magnetic order or perhaps even the superconductivity in the high T_c materials can be substantially increased. Moreover, the mere fact that U and Δ become smaller also implies that the conductivity gap will be reduced.

2.3. Madelung potentials

From the XPS study, we have found that the core level spectra of MgO(100) films shift progressively towards lower binding energy with decreasing thickness [6]. It would be valuable if such shifts can be directly related to changes in the ionization potentials or Madelung potentials. This is relevant for the understanding of the changes that might occur in various chemical and physical properties of oxide–metal interfaces with film thickness. However, such a one-to-one relation is difficult to make for insulating films, since the measured one-electron removal energies depend on where the chemical potential is positioned inside the band gap.

Table 1
Madelung potentials in a free standing MgO(100) monolayer, in a free standing unrelaxed MgO(100) doublelayer, at the (100) surface of bulk MgO, inside the MgO bulk, and in a free standing MgO(100) double layer with a 20% smaller interlayer spacing

MgO(100)	V^{Mg}_{Mad}	V^{O}_{Mad}	$2\delta V_{Mad}$
Monolayer	−22.092	22.092	−3.612
Unrelaxed doublelayer	−23.005	23.005	−1.786
Surface of bulk	−22.994	22.994	−1.808
Inside bulk	−23.898	23.898	0
20% compressed doublelayer	−24.329	24.329	0.862

The $Mg^{2+}O^{2-}$ lattice constant is 4.212 Å. $2dV_{Mad}$ is the difference in $2|V_{Mad}|$ relative to the inside bulk value. All values are in V.

The problem is that the chemical potential is usually pinned by defects, the nature and concentration of which are very sensitive to details of the preparation conditions. The chemical potential position can therefore vary strongly from sample to sample. To obtain the required information, we have done [6] the analysis using the Mg 1s core level as an internal reference of the MgO(100) film itself. In this way we found that the Madelung potential of 1 ML MgO(100) on Ag(100) is reduced by $2dE_{Mad}$–1.0 eV as compared to the bulk value [6]. This result shows that in going from the bulk situation to the monolayer on a metal system the ionization potentials of the MgO films, and consequently also charge transfer energies, are modified not only due to the increase of the extra-atomic relaxation energies but also due to the reduction of the Madelung potential.

For a quantitative understanding, we can calculate the Madelung potential in the overlayer using the simple classical image charge model as a start to account for the metal substrate contribution. Let us assume that the MgO–Ag interlayer spacing is the same as that of the MgO layers in bulk MgO, and that the image plane is located half way between the cores of the MgO ions and Ag atoms. Then the overlayer forms effectively with its image a free standing unrelaxed MgO(100) double layer system. We have calculated the Madelung potential for this, and found that it is larger than for a free standing MgO(100) monolayer, but smaller than for the bulk. Interestingly, it is almost identical (within 0.05%) with that of the (100) surface of solid MgO. The results are summarized in Table 1. Using 2+ and 2– charges for the ions, we obtain $2dE_{Mad} = -1.786$ eV for the unrelaxed double layer (this quantity is the difference in $2E_{Mad}$ between the double layer and the bulk). The calculated reduction of the Madelung potential is nevertheless too large in comparison with the experiment ($2dE_{Mad}$–1.0 eV, see above). In other words, the contribution of the metal substrate to the Madelung potential of the overlayer is underestimated: the contribution to $2E_{Mad}$ is 1.826 eV as can be found from Table 1 when comparing the double layer with the monolayer. We note, however, that the computational results depend strongly on the exact position of the image plane. Placing the image plane of the Ag(100) surface at, for instance, 1.26 Å above the cores of the Ag surface atoms, as suggested from an analysis of image potential surface states on clean Ag(100) surfaces [9], the overlayer system then corresponds to a MgO(100) double layer system with an approximately 20% compressed interlayer spacing. As shown in Table 1, we then find $2dE_{Mad} = +0.862$, which means that now the metal substrate contribution is overestimated: the contribution to $2E_{Mad}$ is 4.474 eV as can be derived from the difference with the monolayer. A correction can possibly be made by considering the fact that the image potential will deviate from the $1/r$ behavior for these short distances [10–12], and that the Mg and O ions in the overlayer may have less charge than in the bulk. Although such a classical approach is expected to break down in view of the atomistic nature of the metal surface so close to the interface, [13–15] the simple analysis shows at least that it is a priori not obvious that the Madelung potential of the overlayer is smaller than in the bulk, and that a measurement is needed to determine it.

3. Non-correlated oxide thin films on metals

The properties of *non-correlated* oxides are mainly determined by electron delocalization and hybridizational effects. Therefore, for these material the reduction of U and Δ in the vicinity of a metal surface are not so much relevant. Nevertheless, also non-correlated oxide thin films on metals might have an electronic structure, and perhaps also chemical properties, which greatly deviate from those of the bulk materials and their surfaces, mainly because of the reduced coordination, the symmetry breaking, and the possible hybridizational interactions with the metal surface. For example, the reduced surface Madelung potential, together with the hybridizational effect between the oxide and the metal, may result in the development of interfacial mixed density of states, over the energy region of concern for various chemical interactions, i.e. the low energy scale close to the Fermi level, perhaps stabilizing chemical reactions energetically unfavored at the surface of bulk oxides. This is shown in Fig. 4 reporting the photon energy dependence of the photoelectron spectra measured from 1 ML MgO(100)/Ag(100), the clean Ag(100), and polycrystalline Ag, excited with photon energies of 21.2 eV (He I, panel a), 40.8 eV (He II, panel b), and 1486.6 eV (Al K_a, panel c), respectively [16]. The bottom panels display the corresponding difference spectra. Here, the important features are those located between 4 eV binding energy and the Fermi level. These features exhibit a clear trend if we compare the spectra taken at the three photon energies: the magnitude of the difference between the MgO covered and clean Ag spectra decreases dramatically with increasing photon energies, even if we include a correction for the fact that the probing depth for the Al K_a measurement is 3 times larger than that for the He I and He II experiments. This trend coincides nicely with the photon energy dependence of the photoionization cross-section [17] of the O $2p^6$ relative to that of the Ag $4d^{10}$: $s(O\ 2p^6)/s(Ag\ 4d^{10}) = 1.0$, 0.3 and 0.02 for $h\upsilon =$ 21.2, 40.8, and 1486.6 eV, respectively. This indicates that the features appearing in the MgO/Ag interface spectra between 4 eV binding energy and the Fermi level have a strong O 2p character, and that these O 2p states are spread out that much in energy due to the strong hybridization with the wide Ag 5sp band [16].

It is interesting to note that the O 2p derived states exhibit a clear Fermi cut-off (see bottom panel of Fig. 4a), demonstrating that there are also O 2p derived states pushed above the Fermi level by the interaction with the Ag 5sp [16]. The strong metallic character of the interfacial oxygen atoms is the most important feature of the MgO(100)/Ag(100) interface electronic structure, since only the low energy scale is relevant to many ground state properties and chemical–physical processes and applications. The bonding mechanism and the binding energy of the MgO(100)/Ag(100) interface, for instance, are determined by those mixed antibonding states that are pushed above the Fermi level, thereby lowering the total energy of the system. Moreover, the chemistry of the oxide–metal interface will be strongly influenced by the presence of oxygen states in the vicinity of the Fermi level, because these states can hybridize with the orbitals of the adsorbed species. As a result, the activation energies for some specific chemical reactions may be altered, and also chemical species may now be formed which would not have been stable on surfaces of the bulk oxide material. Moreover, the presence of the metal substrate may also significantly influence the chemical reactivity also in another way. In fact, as discussed in the previous section, in the close proximity of the oxide–metal interface, ionization potentials are reduced and affinity energies increased by approximately 1 eV [6] due to the efficient image charge screening. This in turn means that the activation energy barrier for various dissociation processes can be lowered, thereby effectively enhancing the chemical reactivity.

Support for the above ideas can be found in the dramatic reactivity of the MgO(100)/Ag(100) interface, demonstrated by the strong spectral modifications occurring in the Mg and O core levels. This is exemplified in Fig. 5 displaying the O 1s core level XPS spectra for the MgO(100) monolayer on Ag(100) measured at different times after the film growth [16]. Immediately after the film growth (thin line), the O 1s spectrum consists of a single line. However, after prolonged exposure to the residual gas in the XPS spectrometer,

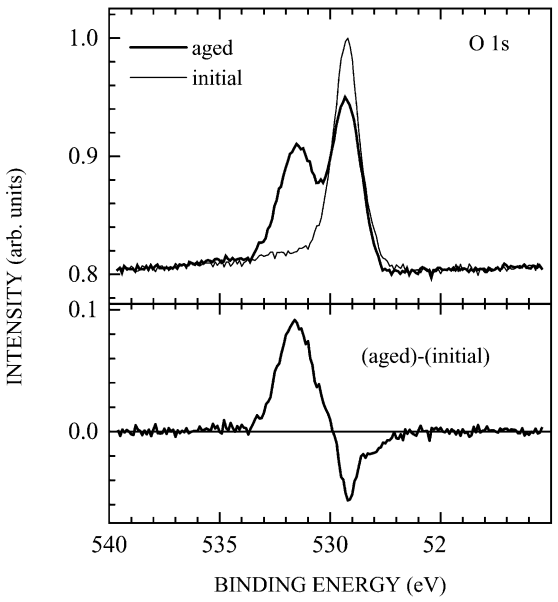

Fig. 5. Top panel: O 1s core level XPS spectra from the MgO(100) monolayer on Ag(100), immediately after the film growth (thin line) and after complete ageing (thick line). Bottom panel: difference between the aged and initial spectra.

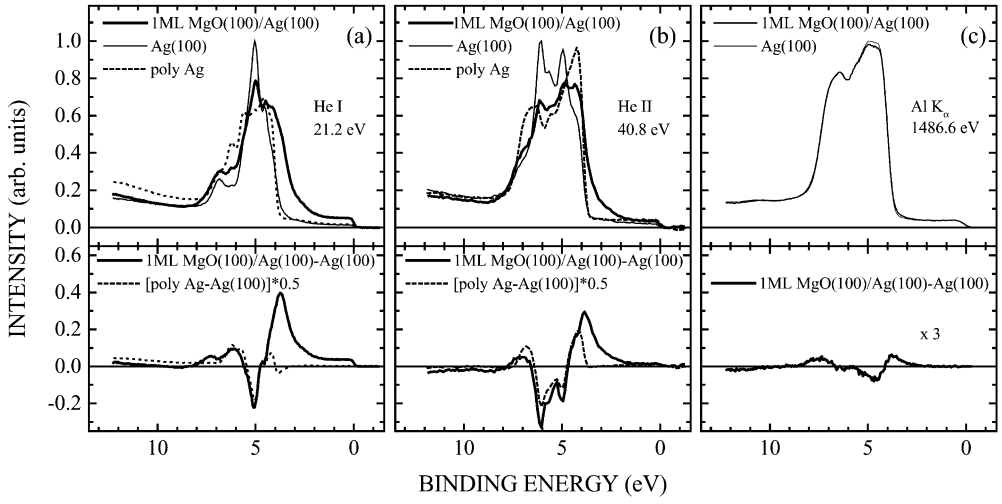

Fig. 4. Valence band photoemission spectra from the MgO(100) monolayer on Ag(100) (thick lines), from the clean Ag(100) surface (thin lines), and from a polycrystalline Ag sample (dashed lines), taken with (a) He I ($h\upsilon = 21.2$ eV), (b) He II ($h\upsilon = 40.8$ eV) and (c) Al K_a ($h\upsilon = 1486.6$ eV) photons. The three top panels show the individual spectra, and the three bottom panels depict the difference spectra: the difference between the MgO covered and the clean Ag(100) surface (solid lines), and the difference between the polycrystalline and the (100) Ag surface (dashed lines). The He I and He II spectra are recorded at normal emission, and the Al K_a spectra at 55° from the surface normal.

an intense satellite appears at 2.3 eV higher binding energy (thick line). The appearance of the O 1s satellite is accompanied by a consistent decrease of the O 1s main line by approximately 25%. However, the ratio of the satellite increase to the main line decrease is in the range 2.5:1 to 3.5:1, thereby demonstrating an overall increase of the oxygen content in the ageing film. Interestingly, the observed ratio of the satellite intensity increase to main line intensity decrease is consistent with the ratio of 2:1 expected for H_2O dissociative chemisorption at the MgO(100)/Ag(100) interface [16]. On the contrary, dissociative chemisorption of H_2, which might equally produce the appearance of a O 1s satellite, is ruled out by the result of Fig. 5, since the latter chemical reaction would lead to a satellite increase to main line decrease of 1:1 [16]. Furthermore, the absence of C 1s signal from the fully aged film [16] indicates that the MgO(100)/Ag(100) interface does not react, at least not in a simple way, with CO and CO_2 molecules.

We remark that the O 1s experiment shown in Fig. 5 is not a clear-cut one, and dosing of a well-defined amount and type of gas, in combination with, for example, high resolution electron energy loss experiments, would be much more instructive. Moreover, a detailed characterization of the structure and defectivity of the MgO(100)/Ag(100) interface is required to evaluate the role of defects and low coordinated sites on the chemical properties of the oxide–metal interface. Nevertheless, the present results strongly suggest that the oxide/metal interface have rather peculiar chemical properties very different from those of the surfaces of the bulk oxide. This in particular can be understood realizing that both defects and low coordinated sites at the surface of a bulk oxide have similar affinity for molecules such as H_2O, H_2, CO and CO_2, while the MgO(100)/Ag(100) seems to selectively and efficiently react only with H_2O and not with other molecules. We argue that such a peculiar reactivity is closely related to the special electronic structure of the oxide/metal interface [16].

4. Conclusions

We have discussed some basic ideas connected with intriguing interfacial phenomena which might lead to unprecedented properties at oxide–metal interfaces. Results on the MgO(100)/Ag(100) interface taken as a model system are consistent with these ideas, and strongly suggest that ultrathin oxide films on metals and oxide/metal interface may indeed have unique chemical–physical properties due to the mutual interactions between the oxide and the metal.

References

[1] H.-J. Freund, H. Kuhlenbeck, V. Staemmler, Rep. Prog. Phys. 59 (1996) 283.
[2] H.-J. Freund, Phys. Stat. Sol. (b) 192 (1995) 407.
[3] S.A. Chambers, Surf. Sci. Rep. 39 (2000) 105.
[4] D.W. Goodman, J. Vac. Sci. Technol. A 14 (1996) 1526.
[5] D.M. Duffy, A.M. Stoneham, J. Phys. C 16 (1983) 4087.
[6] S. Altieri, L.H. Tjeng, F.C. Voogt, T. Hibma, G.A. Sawatzky, Phys. Rev. B 59 (1999) R2517.
[7] S. Altieri, PhD Thesis, Groningen, 1999.
[8] L.H. Tjeng, H. Eskes, G.A. Sawatzky, in: H. Fukuyama, S. Maekawa, A.P. Malozemoff (Eds.), Springer Series in Solid State Sciences, vol. 89, Springer Verlag, Berlin, Heidelberg, 1989, pp. 33.
[9] N.V. Smith, C.T. Chen, M. Weinert, Phys. Rev. B 40 (1989) 7565.
[10] P.M. Echenique, J.B. Pendry, J. Phys. C 11 (1978) 2065.
[11] R.O. Jones, P.J. Jennings, O. Jepsen, Phys. Rev. B 29 (1984) 6474.
[12] N.V. Smith, Phys. Rev. B 32 (1985) 3549.
[13] P.B. Jennings, R. Jones, Adv. Phys. 37 (1988) 341.
[14] D.M. Duffy, J.H. Harding, A.M. Stoneham, Philos. Magaz. A 67 (1993) 865.
[15] M.W. Finnis, J. Phys. C 8 (1996) 5811.
[16] S. Altieri, L.H. Tjeng, G.A. Sawatzky, Phys. Rev. B 61 (2000) 16948.
[17] J.J. Yeh, I. Lindau, At. Data Nucl. Data Tables 32 (1985) 1.